Available online at www.sciencedirect.com

ScienceDirect

Energy Procedia 148 (2018) 98–105

Energy Procedia

www.elsevier.com/locate/procedia

73rd Conference of the Italian Thermal Machines Engineering Association (ATI 2018), 12–14 September 2018, Pisa, Italy

Numerical Study of Flutter Stabilization in Low Pressure Turbine Rotor with Intentional Mistuning

Sara Biagiotti[a]*, Lorenzo Pinelli[a], Francesco Poli[a], Federico Vanti[a], Roberto Pacciani[a]

[a] *Department of Industrial Engineering, Università degli Studi di Firenze, Via di Santa Marta 3, 50139 Firenze, Italy*

Abstract

Intentional mistuning concepts are used to mitigate the risk of flutter occurrence for compressor and turbine blades, as this design strategy represents one of the key aspects in nowadays turbomachinery aeroelastic design. In this paper, the effects of a mistuning pattern on LPT flutter stability are numerically investigated in order to highlight the differences with the classic *tuned* configuration. A LPT rotor is analysed with an intentional mistuning pattern composed by alternate blades with different additional masses at the blade tip, and the corresponding *tuned* configuration, consisting of the blisk (blade+disk) with identical blades. The first part of this work is devoted to the modal analysis for *tuned* and *mistuned* cases. Frequencies and mode shapes of the first bending mode family, obtained by FEM modal analysis in cyclic symmetry, are then used to perform CFD flutter analysis with moving blades. The results confirm the stabilizing effect of *alternate* mistuning pattern in contrast with the *tuned* system which denotes a strong flutter instability for a large range of negative nodal diameters. The numerically predicted flutter stabilization effect has been confirmed by measurements carried out during a tip timing experimental campaign performed within the *Future* EU project.

Keywords: low pressure axial turbine; aeroelasticity; flutter; mistuning; FEM; CFD

* Corresponding author. Tel.: (+39)055-275-8795; fax: (+39)055-275-8755.
E-mail address: sara.biagiotti@tgroup.unifi.it

1876-6102 © 2018 The Authors. Published by Elsevier Ltd.

10.1016/j.egypro.2018.08.035

1. Introduction

In modern turbomachinery design, the continuous research for increasing performance, efficiency and reliability while lowering costs, has led to a reduction of the number of mechanical parts and to design thin and highly loaded blades. This trend significantly increases the relevance of aerodynamically induced vibration phenomena, such as flutter and forced response, compromising the structural integrity. For this reason, aeroelasticity has become one of the critical aspects of turbomachinery blade design: assessing whether a blade row will experience flutter or forced vibrations under given operating conditions is an important part of the design activity. It is therefore essential to numerically evaluate the flutter response of turbine blade rows with CFD methods. In the last decades, many numerical approaches have been developed to help a flutter free design. Such methods have become more and more accurate, as computing power has increased [1] [2] [3] [4]. In this context, *intentional mistuning* becomes a design strategy that permits to reduce flutter induced vibrations or better to stabilize the flutter unstable blade row. Different types of mistuning exist: an intentional modal and geometrical mistuning can be included in turbine rotor rows by modifying inertial and geometrical properties of adjacent profiles usually with a well-defined circumferential pattern. Modal mistuning consists of changing blade mode shapes and their natural frequencies without modifying the aerodynamic blade surfaces, whereas geometrical mistuning aims to modify the geometry of the adjacent blades and, in turn, the mode shape. This latter design concept can stabilize flutter induced blade vibration, but on the other hand, it also influences the blade aerodynamic performance, usually decreasing the efficiency. In the aeroelastic research field, many works [4] [5] confirm the beneficial effects for the flutter stabilization, especially when alternated mistuning is somehow introduced. It is also well-known that this design strategy has a detrimental effect on the rotor forced response. Anyway, due to the high risk of the flutter onset for LPT rotor it is preferable to include mistuning in rotor design.

Nomenclature

a	Modal amplitude
E	Kinetic energy
m	Modal mass
nd	Number of nodal diameter
W_{aero}	Aerodynamic work

<u>*Acronyms*</u>

BTT	Blade Tip Timing
IBPA	Inter Blade Phase Angle
NS	Navier-Stokes
PS	Pressure Side
SS	Suction Side

<u>*Greek Letters*</u>

ξ	Energetic damping coefficient or critical damping ratio
ρ_ξ	Energetic damping coefficient surface density
Σ	Blade surface
ω	Vibration angular frequency

2. CTA test-case

The numerical activity included in this paper is dedicated to a selected test-case based on a LP turbine blade rotor tested at the Centro de Tecnologías Aeronáuticas CTA (Bilbao, Spain) in the context of the *Future* European project. The test rig includes an isolated bladed rotor composed by 146 blades subjected to the incoming flow conditions coming from a far VIGVs (Variable Inlet Guide Vanes). This configuration was selected to study classical flutter phenomenon avoiding as much as possible forced response vibrations caused by upstream and downstream rows. The operating point under investigation (OP1) has a rotational speed of 2773 rpm with a mass flow of 14.42 kg/s.

This blade-row was firstly tested in the *tuned* configuration, designed to experience flutter instability. Then, the *intentionally mistuned* pattern, consisting of alternate masses at the blade tip (see Fig. 1 (d)), was included in order to demonstrate flutter stabilization of the entire row. The flutter instability of the *tuned* configuration is mainly due to the steady blade load (high loaded profile), and to the low vibration frequency of the 1st mode shape (all the blades are made of aluminum). The CTA rotor blade assembly is composed of fir tree attachment, shank, platform, airfoil and tip shroud. The tip shroud design was driven by several non-conventional constraints, as shown in Fig. 1 (b). To excite the rotor blisk for forced response investigations, a permanent magnet is inserted in a cage, fixed to the rotor blade through a single screw. A mistuning mass housing, located between the small fence intended to trigger the optical signal of the blade tip timing system, is inserted to add mistuning mass and so to modify the rotor blade frequency. In addition, a balancing mass has been foreseen to balance the rotor and it is screwed to one of the two small fences used to trigger the blade tip timing signal. Finally, inlet and outlet boundary conditions of the row were acquired using fast response five-hole miniaturized probes that are radially and azimuthally traversed across a distance equivalent to several rotor blade pitches [7]. Blade vibration amplitude measurements were performed using a blade tip timing (BTT) optical system pointed towards the rotor shroud [5]. Unsteady pressure transducers were flush-mounted in the outer casing one chord downstream of the rotor blade to correlate rotor vibration amplitudes with unsteady pressure measurements. [7].

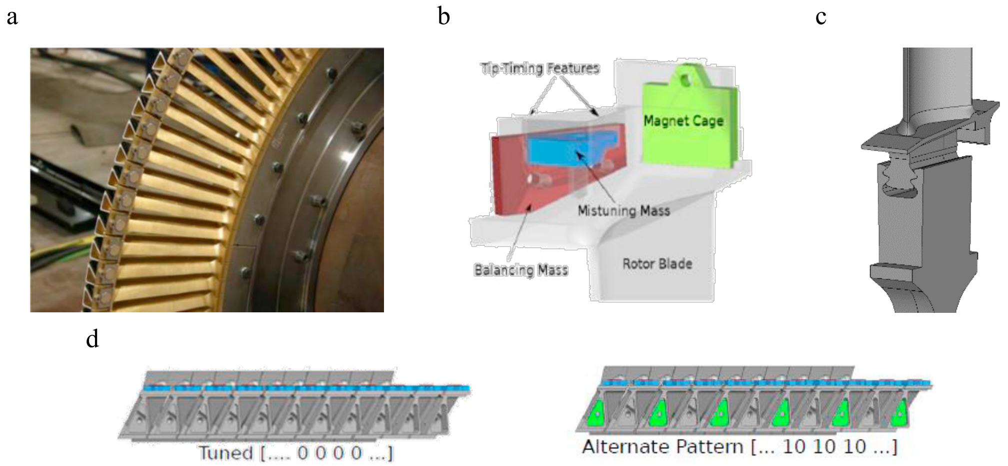

Fig. 1: (a) Rotor blade assembly; (b) Tip-shroud rotor blade; (c) Fir-tree connection; (d) *Tuned* configuration and *alternate mistuning* pattern

3. Blisk discretization and modal analysis

Before performing the discretization of the computational solid domain, it is necessary to pay attention to the rotor blade assembly geometry. All the geometrical features described previously, concerning hub and tip of the blade rotor, must be included in the CAD model in order to keep geometry and inertial characteristics as realistic as possible.

The discretization of the blisk sector of the CTA rotor has been carried out using the Open Source meshing tool available in *Salome* software suite. The solid mesh discretizes the computational domain used to perform a modal analysis with a FEM solver. The solid grid selection has been generated by setting limits to the total elements number and to their minimum size, with the aim of minimizing computational costs while maximizing the mesh accuracy. The 3D mesh is constituted by 110000 quadratic elements of tetrahedral shape. A large number of nodes is positioned at the hub and tip fillet regions and also in the fir-tree connection in order to ensure a good mesh accuracy, being careful of not modifying the stiffness of the system. As the first step, the CAD assembly has been divided in each component to ensure continuity of the solid mesh. Secondly, sets of geometric groups have been created in the discretized model and consequently exported as subsets to impose constraints during modal analysis. Similarly, the *mistuned* rotor basic sector has been discretized as a sector of two blades where cyclic symmetry conditions will be applied considering 73 sectors. The mesh is obtained with the same algorithm and consists of about 300000 quadratic tetrahedral elements. Modal analysis has been performed for *tuned* and *mistuned* configurations with the Open Source FEM solver *CalculiX* in order to compute the first rotor natural frequencies and mode shapes. Boundary conditions used for free response analysis, can be applied exploiting surface and node groups already defined in meshing tool *Salome*.

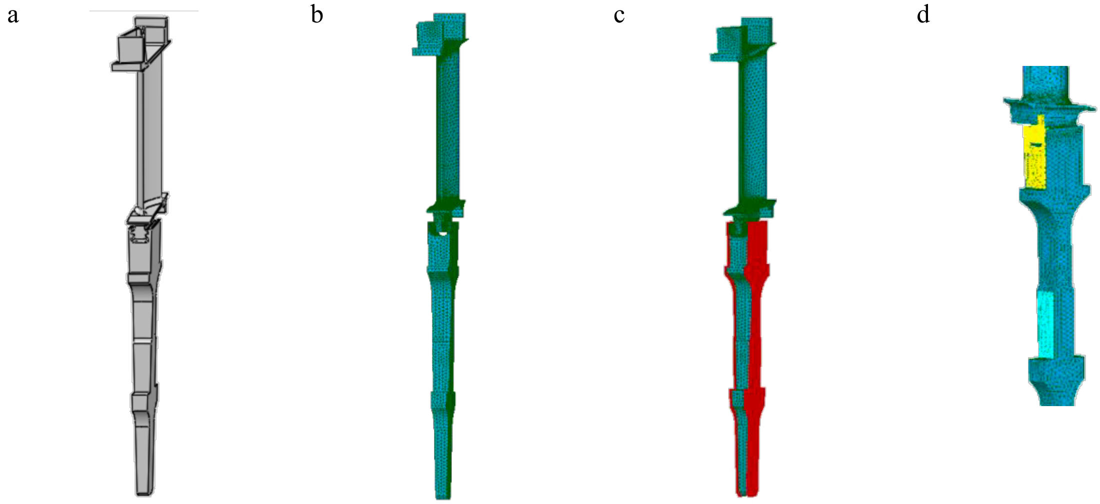

Fig. 2: (a) Disk sector geometric model; (b) Sector 3D mesh; (c) Cyclic symmetry boundary conditions; (d) Axial and tangential constraints

A surface group at the circumferential extremities of the 1- or 2-passage sector has been identified for the cyclic symmetry boundaries on the right and left side of the disk respectively, in order to reduce the computational cost compared with a full structure analysis (Fig. 2 (c)). Then, a group of nodes has been selected to reproduce the axial locking of the blade (yellow nodes in Fig. 2 (d)) and the screw connection between the rotor and two lock plates modelled by an axial and tangential constraint (blue nodes in Fig. 2 (d)). Modal results in terms of frequencies and mode shapes are in agreement with experimental data and are used as an input for the unsteady flutter analyses to deform the CFD domain.

4. Flutter results

Before investigating flutter assessment, steady analyses were carried out in order to evaluate the main aerodynamic characteristics and to match the average flow quantities acquired during the flutter campaigns (such as mass flow, radial profile downstream of the rotor, etc.) to accurately reproduce the operating condition under investigation.

The discretization of the fluid domain has been achieved using a dedicated in-house meshing tool. Both for *tuned* and *mistuned* configurations, the same 3D structured H-type grid has been used since the aerodynamic blade geometry is the same. CFD analysis has been performed using the in-house Traf code which is able to solve the Navier-Stokes equations by using an explicit four stage Runge-Kutta integration algorithm on a cell-centered finite volume discretization of the domain [6]. This solver was firstly extended to perform unsteady computations with vibrating blades thus implementing an aeroelastic solver [1] and later further extended to deal with blade packets deformation to study blade cluster system and *mistuned* rows [2]. In the paper are also included flutter results from the Lars code, which is the time-linearized version of the Traf code, and is used for flutter and tone noise computations. All the details of this time-linearized method can be found in previous publications by the authors [3].

The preliminary steady state analysis was carried out using a k-ω turbulence model, in order to closely match the inlet and outlet quantities such as flow angles, static and total pressure coming from experimental measures of the operating point under investigation. This mean steady solution is also employed to initialize the unsteady analysis with moving blades. Unsteady flutter analysis has been performed with an uncoupled nonlinear method implemented in Traf and by applying phase lagged periodicity conditions, both for *tuned* and *mistuned* configurations. Unsteady pressure response is evaluated over the blade surface while the blade-row vibrates in a travelling wave manner. Once the periodicity has been reached, the unsteady pressure is finally integrated during an oscillation period over the blade surface and the aerodynamic work is computed. Flutter stability is estimated by checking the sign of the critical damping ratio ξ, obtained by the aerodynamic work normalization (see Eq. (1)).

$$\xi = \frac{-W_{aero}}{2\pi m \omega^2 a^2} \qquad 1$$

where W_{aero} is the aerodynamic work, m is the blade modal mass, ω is the angular vibration frequency and a is the modal amplitude. A positive value of this quantity leads to a stable condition since the blade transfers energy to the fluid flow in case the row is vibrating; vice-versa a negative sign denotes an unstable behavior and the blade increases its vibration amplitude by extracting energy from the fluid flow. To deeply understand where the stable/unstable areas are located on the blade surface, energetic damping coefficient surface density ρ_ξ can be computed as follows:

$$\rho_\xi = \frac{-dW_{aero}}{8\pi E \frac{d\Sigma}{\Sigma}} \qquad 2$$

where E is the blade average kinetic energy and Σ is the blade surface. This local quantity can be plotted on the blade surface to highlight the most unstable areas where a blade redesign can be applied.

4.1. Tuned configuration results

The numerical results obtained from modal analyses with cyclic symmetry for the *tuned* configuration are presented in Fig. 3. It can be seen on the left of Fig. 3, where the 1st mode frequency is plotted over nodal diameters, that the natural frequencies are well reproduced and the agreement with the available experimental data is satisfactory. Note that the frequencies are rather constant vs. the nodal diameters, except for *nd = 0* due to a disk participation on the overall structure vibration that leads to a lower stiffness and thus ba lower frequency. For the other nodal diameters, the disk does not participate in the traveling wave vibration and the mode shape is real. On the right of Fig. 3, the modal displacements of the 1st bending mode for *nd = 0* (standing wave deformation) and *nd = 60* are shown. The two mode shapes are almost similar, yet it can be noticed that blade deformation for *nd = 60* is located at higher radii.

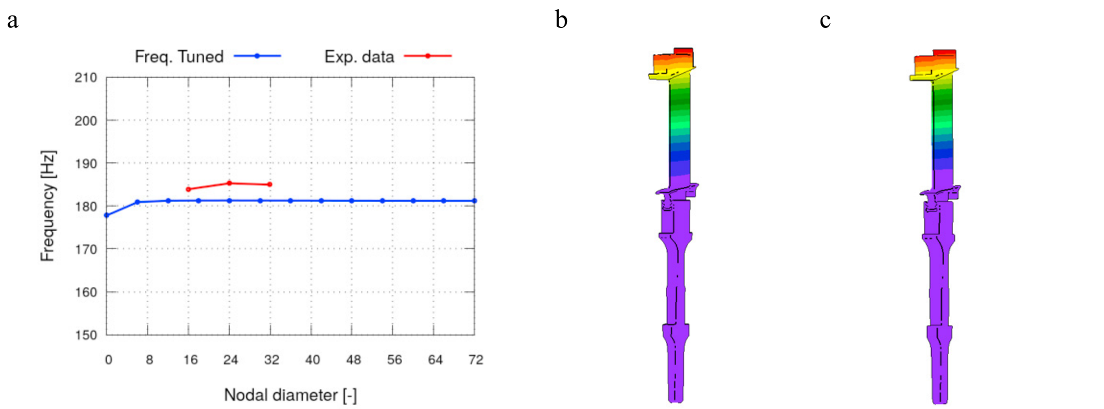

Fig. 3: (a) Frequency distributions vs. experimental data; Global modal displacement for first bending mode (b) *nd* = 0 (c) *nd* = 60

The above-mentioned modal analysis results obtained by *CalculiX* are used only for the non-linear flutter analysis, whereas the mode shapes for the time-linearized computations were previously obtained from a validated commercial FEM code. This aspect allows a direct comparison between two different FEM solvers in terms of frequency and mode shapes and also in terms of flutter results in order to validate the modal analysis approach based on the Open Source *CalculiX* code. As already stated, flutter stability is estimated by checking the sign of the energetic damping coefficient applied by the fluid onto the blade during one vibration cycle when the unsteady solution reaches the periodicity. A periodic solution is obtained when the aerodamping and blade loads stay very close between consecutive periods and for this analyses with the non-linear solver Traf, 10 blade vibration periods were needed to reach the required solution periodicity. On the other hand, the convergence of the time-linearized code is checked by looking at the residual as for a steady state computation. The computational time of flutter analyses depends on the numerical method: a time-linearized for a single nodal diameter takes about 1 h using 8 cores, whereas the computational time for the non-linear method with the same setup is about 5 h. As expected the critical damping ratio curves for the first bending mode in *tuned* configuration (Fig. 4 (a)), computed for selected nodal diameters, shows a sinusoidal trend and highlights a flutter instability for a large range of negative nodal diameters. The two solvers predict similar aerodamping curves although the modal analysis was performed with different solvers which provided slightly different mode shapes. This also means that non-linear effects are not important for the flutter response of this test-case where the flow is subsonic and non-linear phenomena, like shock waves and detached flows, are not present in the flow field. From numerical results, the most unstable nodal diameter corresponds to *nd* = –30. The experimental free-flutter test campaign, carried out during the *Future* EU project, confirms the numerical predictions presented herein. A higher blade instability is detected by a tip timing acquisition technique for the 1st bending mode and from the experimental data it was found that the most unstable nodal diameters were located around IBPA=-90° as correctly predicted by the two solvers. Note that IBPA is related to the nodal diameter value and defined as follows:

$$\text{IBPA} = \frac{2\pi}{N} n \qquad with\ n \in \mathbb{Z}\!:\ -\frac{N}{2} \leq n < \frac{N}{2} \tag{3}$$

It is also possible to display the stable and unstable areas over the blade, using the energetic damping coefficient surface density distribution. In Fig. 4 (b) this local quantity is shown for the most unstable nodal diameter, *nd* = –30, highlighting at tip section a wide unstable zone (in red).

a b

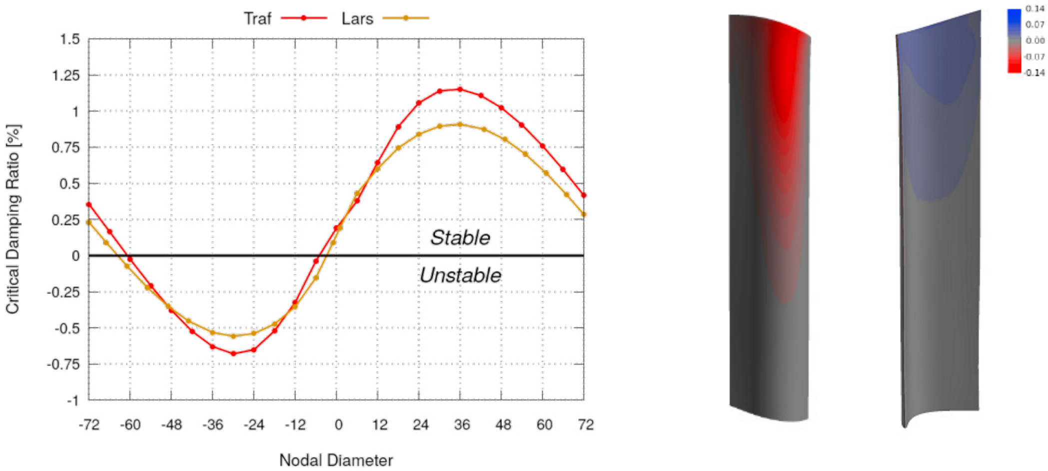

Fig. 4: (a) *Tuned configuration* –Critical damping ratio from time-linearized and non-linear solvers; (b) ρ_ξ for *nd* = -30

4.2. Mistuned configuration results

To study the alternate mistuning configuration obtained by introducing an additional mass at the tip of alternate blades, modal and flutter analyses must be performed on a two-blade sector. The presence of *intentional mistuning* breaks the *tuned* cyclic symmetry and the modal analyses results show that the first bending modes are split into mode shape families. In each family, one blade vibrates more than the other one, with a mode shape similar to the *tuned* configuration (see Fig. 3 and Fig. 5). All the mode shapes with the same nodal diameter and belonging to the two different families have a frequency shift (see left side of Fig. 5): the low frequency corresponds to the mode where the blade with mistuning mass vibrates the most, whereas the high frequency is related to the mode with higher displacements of the blade without the mass. The two 1st bending mode families of the two-blade packet are separately transferred to the two adjacent blades within the NS grid: global displacements of a 2-blade disk packet are shown in Fig. 5.

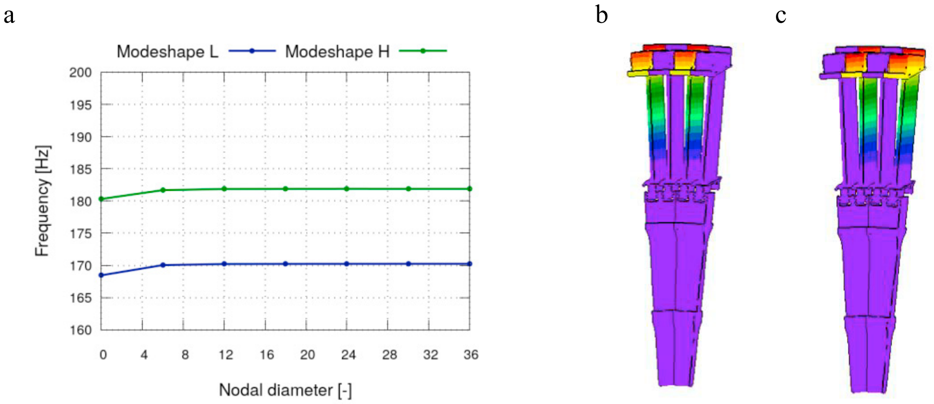

Fig. 5: (a) Frequency distributions for mistuned configuration; (b) Low and (c) high frequencies

The frequency curves for the two 1st bending mode families show a trend similar to the *tuned* configuration with constant values at high nodal diameters. For the *mistuned* configuration the nodal diameters are half of the *tuned* case and are now related to the phase shift between adjacent packets, called IPPA (*Inter Packet Phase Angle*). Critical damping ratio curves (see Fig. 6), one for each family, show the row stabilization due to the introduction of alternate intentional mistuning. This important outcome was experimentally confirmed within the *Future* EU project as the rotor blisk with alternate mistuning pattern did not experience any vibration issue when working at the same operating condition where the *tuned* configuration presents very high vibration level.

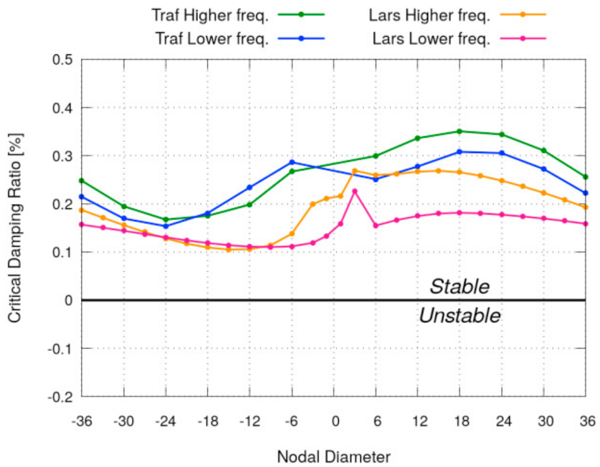

Fig. 6: *Mistuned configuration* – Critical damping ratio from time-linearized and non-linear solvers

As for the *tuned* configuration, time-linearized analyses (Lars) and non-linear computations (Traf) used as input 2-blade packet mode shapes coming from different FEM solvers: a commercial code for time-linearized flutter analyses and the Open Source *CalculiX* solver for the non-linear simulations. The aerodamping curves (for the low and high frequencies) are in agreement between the two solvers, the differences are comparable to the *tuned* configuration. Finally, to highlight the stabilization effect due to mistuning, the ρ_ξ distribution on the vibrating blade for each family with a negative nodal diameter (where single blade configuration is unstable) are shown in Fig. 7. The wide blue areas on the blade PS and SS confirm the overall stability of the mistuned blisk.

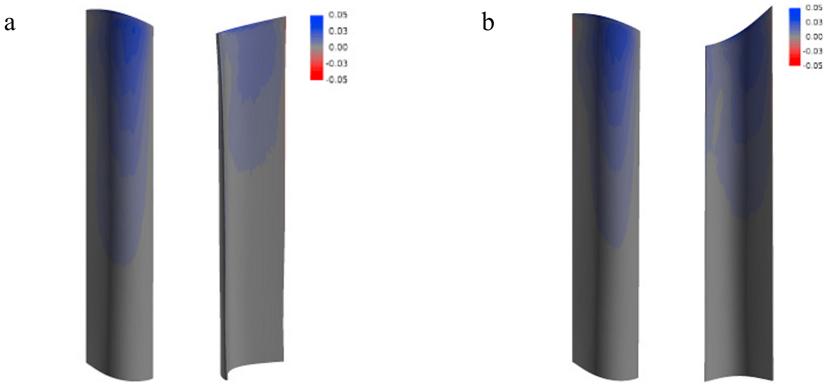

Fig. 7: ρ_ξ for *nd* = -18 mode shape (a) low and (b) high

5. Conclusions

The actual trend in the turbomachinery design entails a continuous increment of the aeromechanical issues. Numerous research programs are dedicated to a better understanding of aeroelastic phenomena in order to design flutter resistant turbomachinery components. The *Future* EU project gave the opportunity to build a few test rigs for turbine and compressor stages dedicated to aeroelastic aspects in order to have a deeper insight on flutter and forced response problems and to provide high quality data for code validation. In this context, a LPT rotor was designed and tested at the Centro de Tecnologías Aeronáuticas CTA (Spain) to experience flutter instability and to verify the blisk stabilization effect due to the introduction of intentional mistuning by adding masses on alternate blades. The flutter assessment of the above-mentioned LPT rotor has been numerically evaluated with two different solvers: a time-linearized code (Lars) and a non-linear approach based on the URANS code Traf. Modal analyses, which provide the input in terms of frequencies and mode shapes, are computed with two different codes: a commercial FEM solver and an Open Source code (*CalculiX*). Firstly, modal analyses have been carried out with the FEM solver for *tuned* and *mistuned* configurations to compute only the first bending mode, which is the most critical for flutter occurrence. The numerical frequencies show an excellent agreement with experimental measurements. Unsteady flutter analyses have been run using the two different codes (Lars and Traf) for selected nodal diameters. The numerical results confirm the high flutter instability detected during the experimental campaign for the *tuned* configuration. On the other hand, the alternate *mistuned* configuration did not experience flutter occurrence during the test campaign. This important experimental evidence was correctly captured by both numerical solvers confirming the accuracy of the two aeroelastic codes and their applicability for flutter resistant blade design.

References

[1] Pinelli L, Poli F, Arnone A, Schipani C. 2009. "A Time-Accurate 3D Method for Turbomachinery Blade Flutter Analysis." 12th International Symposium on Unsteady Aerodynamics, Aeroacoustics and Aeroelasticity of Turbomachines (ISUAAAT). September 1–4, London, UK. Paper I12-S8-3.

[2] Vanti F, Pinelli L, Arnone A, Schneider A, Astrua P, Puppo E. 2018. "Aeroelastic Optimization of an Industrial Compressor Rotor Blade Geometry." ASME Turbo Expo 2018: Turbine Technical Conference and Exposition. Paper GT2018-76474.

[3] Poli F, Gambini E, Arnone A, Schipani C. 2006. "A 3D Time-Linearized Method for Turbomachinery Blade Flutter Analysis." 11th International Symposium on Unsteady Aerodynamics, Aeroacoustics and Aeroelasticity of Turbomachines (ISUAAAT). September 4–8, Moscow, Russia.

[4] Martel C, Corral R, Llorens J. "Stability Increase of Aerodynamically Unstable Rotors Using Intentional Mistuning." Journal of Turbomachinery 130 (2008) 011005.

[5] Corral R, Beloki J, Calza P, Elliot R. "Flutter Generation and Control Using Mistuning in a Turbine Rotating Rig." ASME Turbo Expo 2016: Turbomachinery Technical Conference and Exposition, America Society of Mechanical Engineers, 2016, p. V07BT34A026.

[6] Giovannini M, Marconcini M, Arnone A, Bertini F. 2014. "Evaluation of Unsteady Computational Fluid Dynamics Models Applied to the Analysis of a Transonic High-Pressure Turbine Stage." Proceedings of the Institution of Mechanical Engineers, Part A: Journal of Power and Energy. 228(7):813-824.

[7] Corral R, Beloki J, Calza P, Elliott R. 2016. "Flutter Generation and Control Using Mistuning in a Turbine Rotating Rig." ASME Turbo Expo 2016: Turbomachinery Technical Conference and Exposition. Paper GT2016-57949.